

Supporting Information

Exploring the Potential of Ruthenium(II)-Phosphine-Mercapto Complexes as New Anticancer Agents

*Marcos V. Palmeira-Mello^{a,b}, Analu R. Costa^a, Leticia P. de Oliveira^a, Olivier Blacque^c,
Gilles Gasser^{*b} and Alzir A. Batista^{*a}*

^a Department of Chemistry, Universidade Federal de São Carlos, 13561-901, São Carlos, SP – Brazil.

^b Chimie ParisTech, PSL University, CNRS, Institute of Chemistry for Life and Health Sciences, Paris – France.

^c Department of Chemistry, University of Zurich, Winterthurerstrasse 190, 8057 Zurich, Switzerland.

* Corresponding authors:

Gilles Gasser (ORCID Number 0000-0002-4244-5097) Email: gilles.gasser@chimeparistech.psl.eu, WWW: www.gassergroup.com and Alzir A. Batista (ORCID Number 0000-0002-4671-2754), Email: daab@ufscar.br.

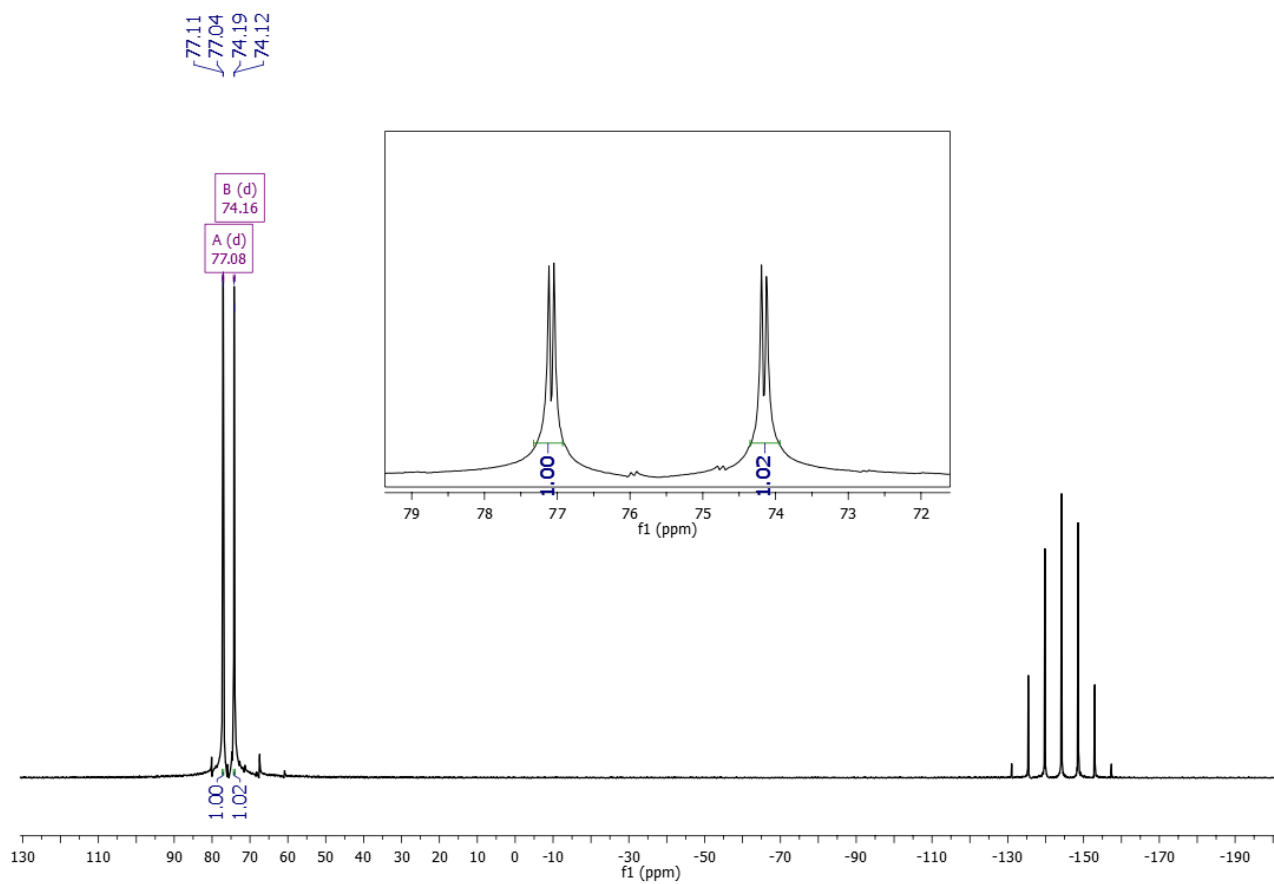


Figure S1. $^{31}\text{P}\{^1\text{H}\}$ NMR spectrum of complex 1 in DMSO-d_6 , 298 K.

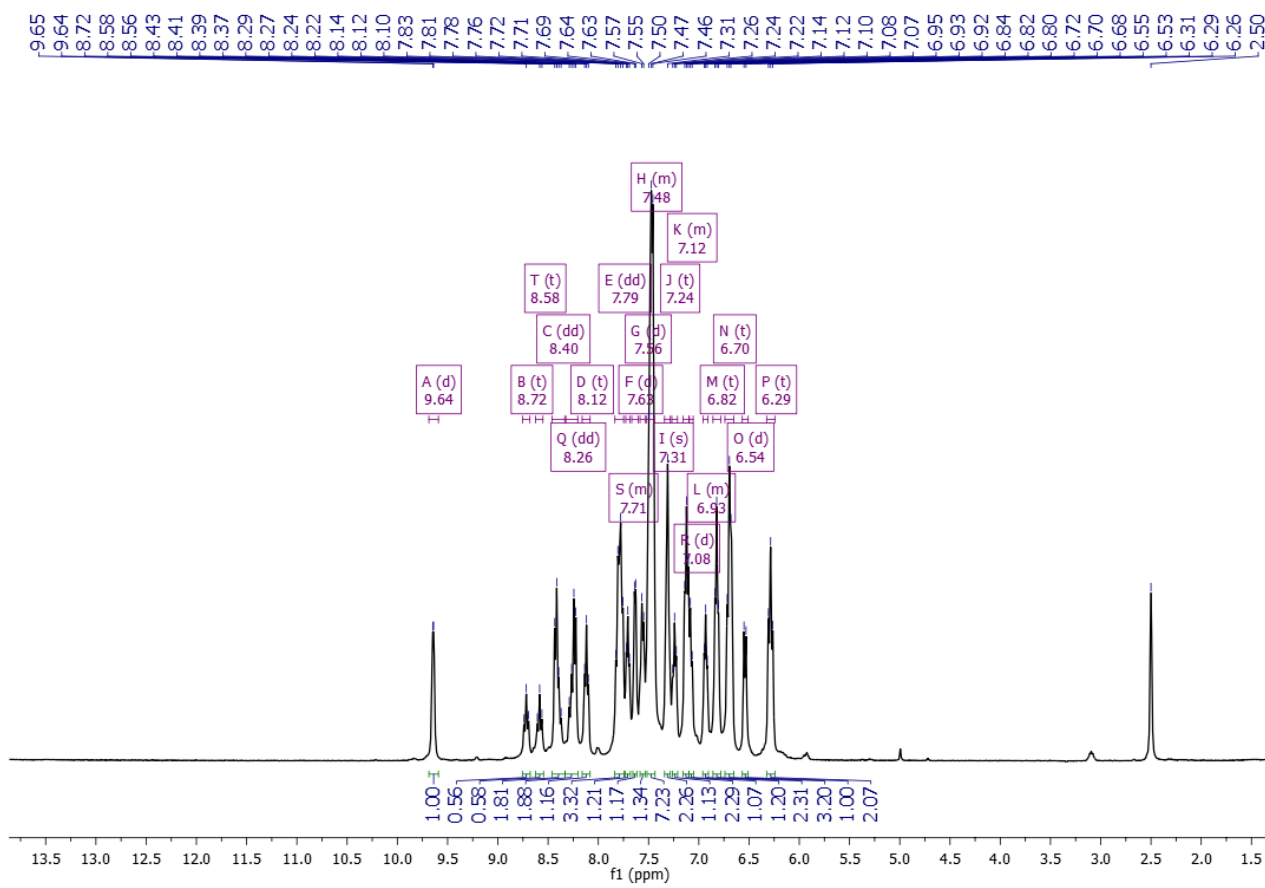


Figure S2. ^1H NMR spectrum of complex **1** in DMSO-d_6 , 298 K.

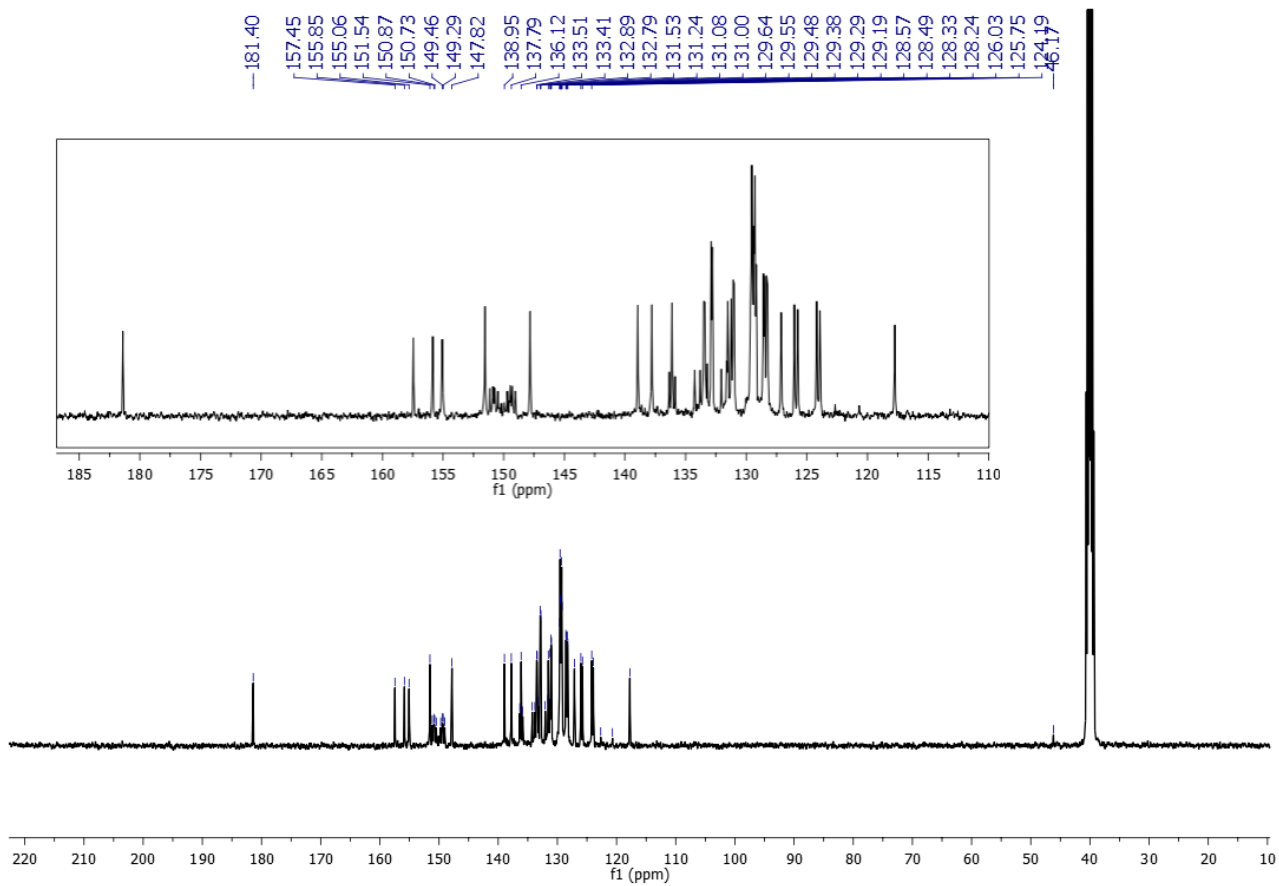


Figure S3. ^{13}C $\{^1\text{H}\}$ NMR spectrum of complex 1 in DMSO-d_6 , 298 K.

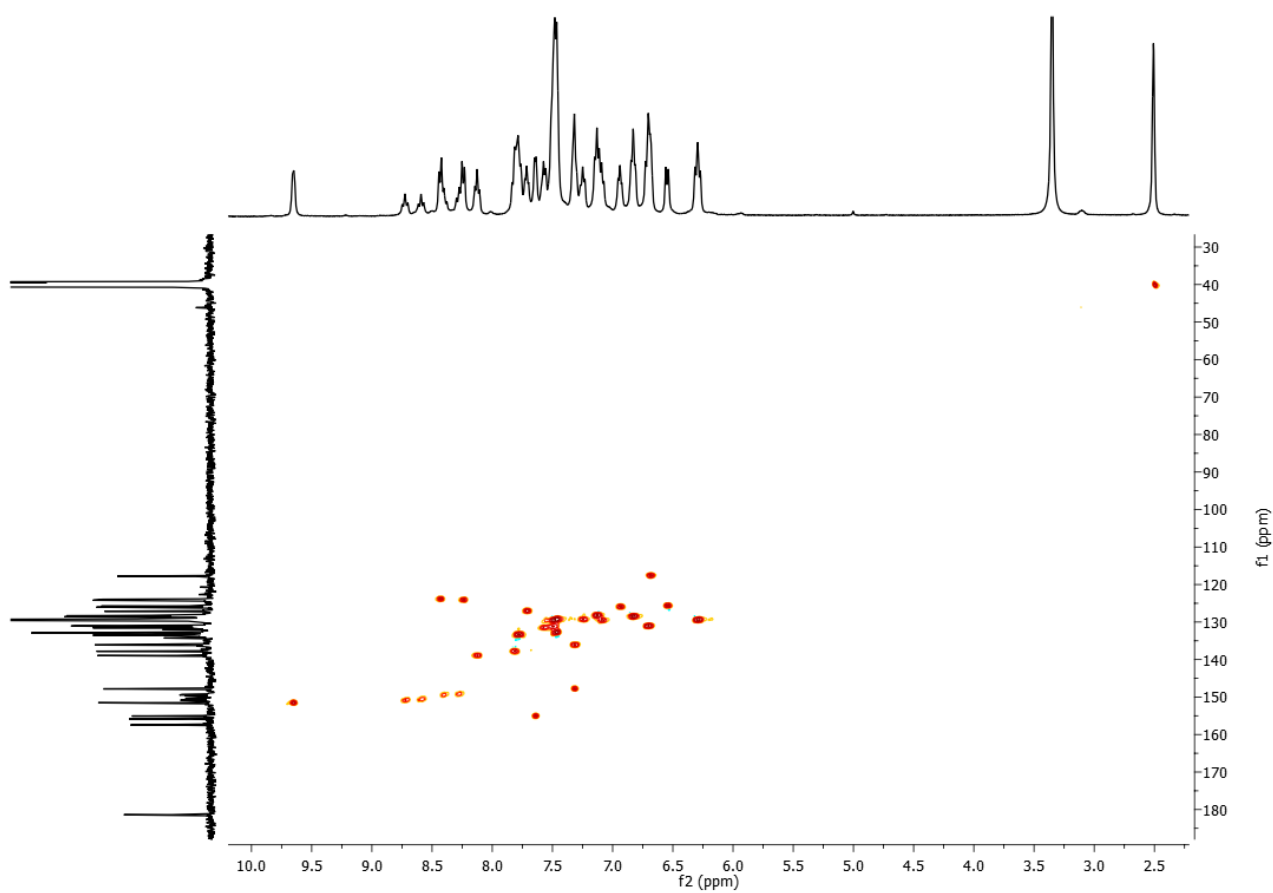


Figure S4. ^1H - ^{13}C HSQC NMR correlation map of complex **1** in DMSO- d_6 , 298K.

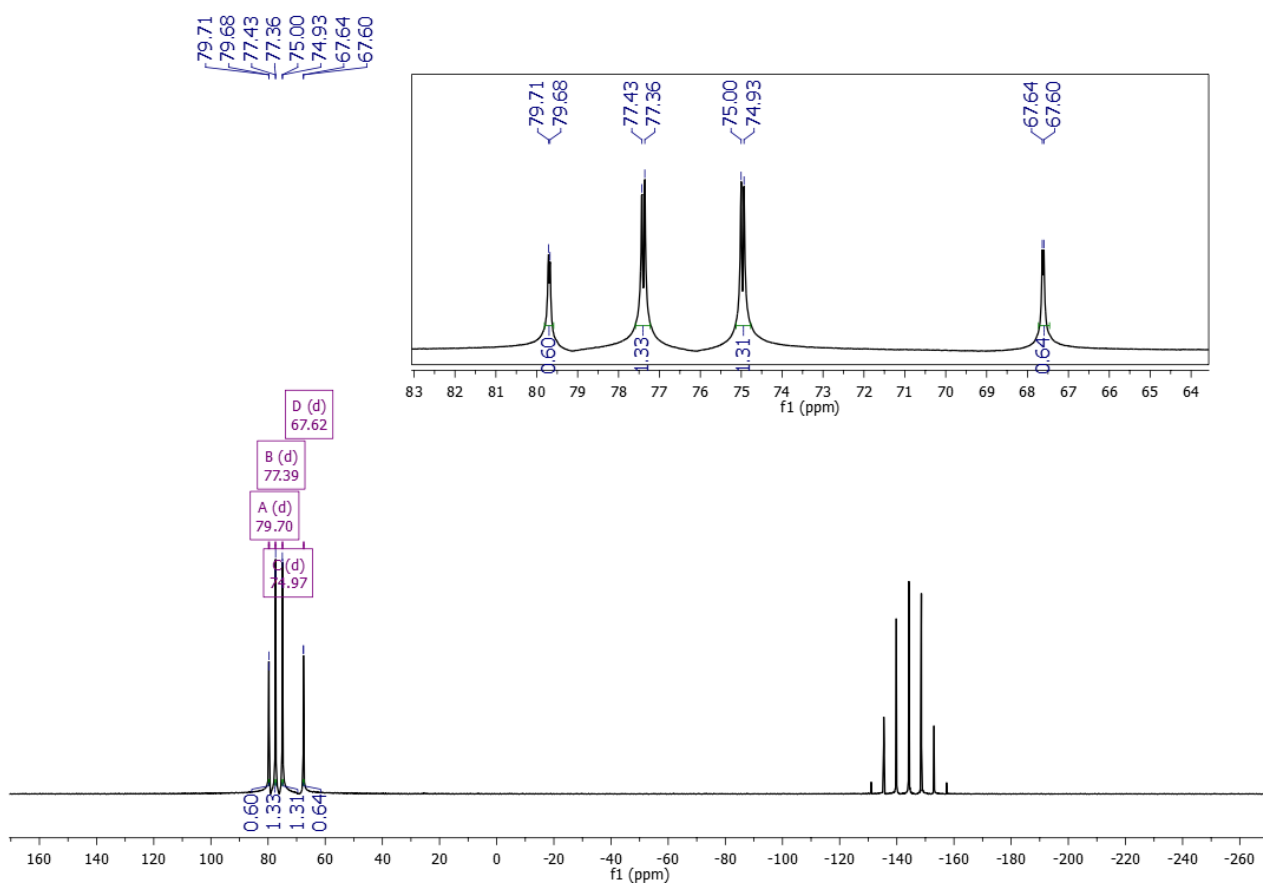


Figure S5. $^{31}\text{P} \{^1\text{H}\}$ NMR spectrum of complex **2a/2b** in DMSO-d_6 , 298 K.

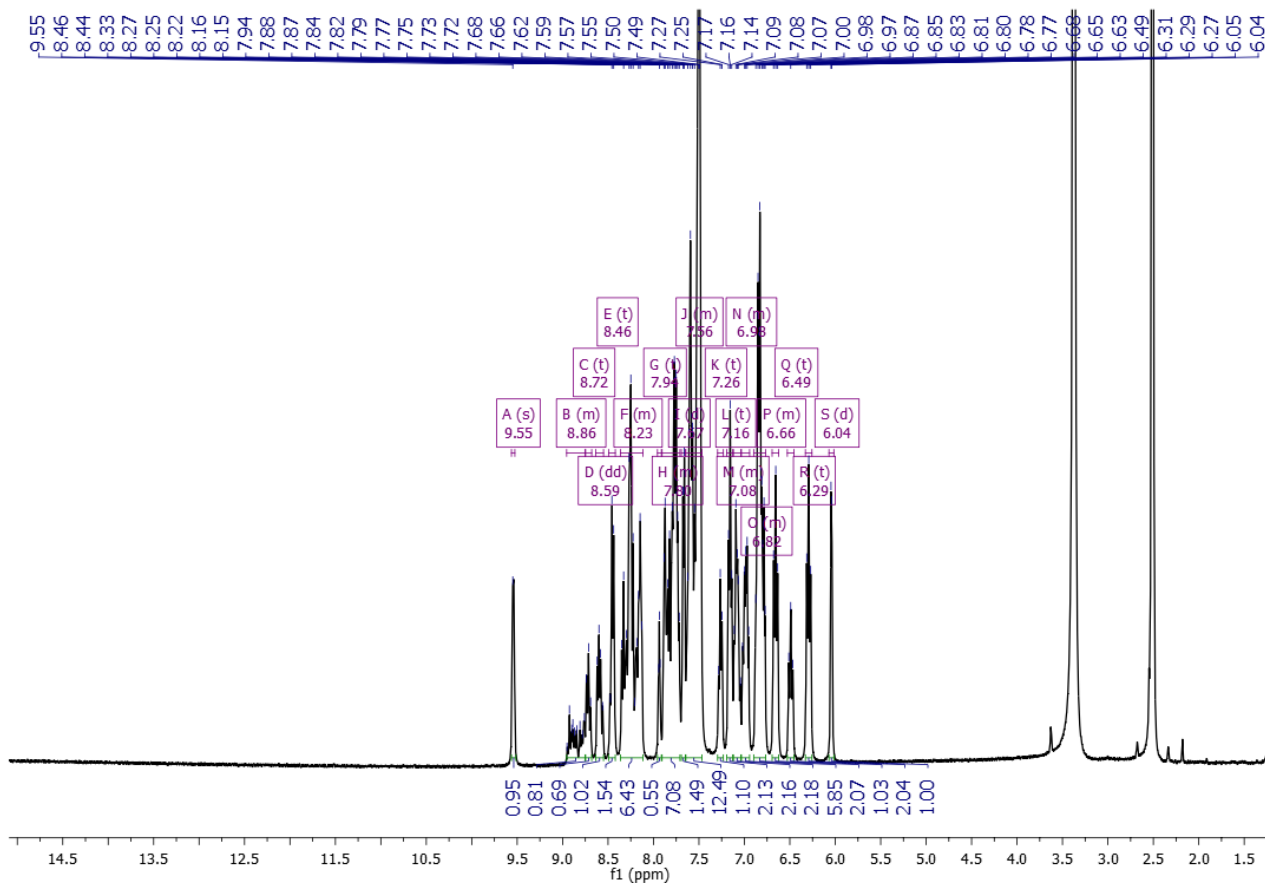


Figure S6. ^1H NMR spectrum of complex **2a/2b** in DMSO-d_6 , 298 K.

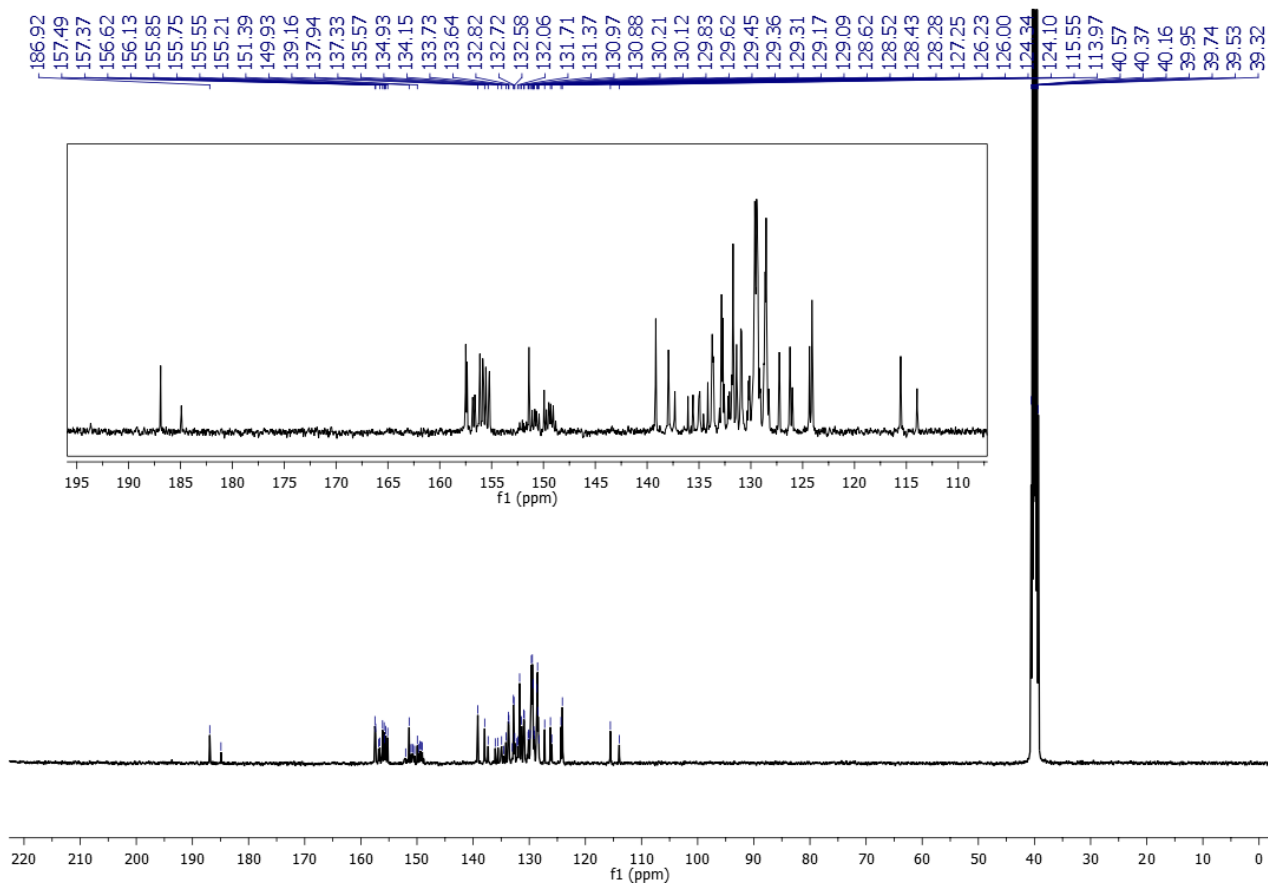


Figure S7. $^{13}\text{C} \{^1\text{H}\}$ NMR spectrum of complex **2a/2b** in DMSO-d_6 , 298 K.

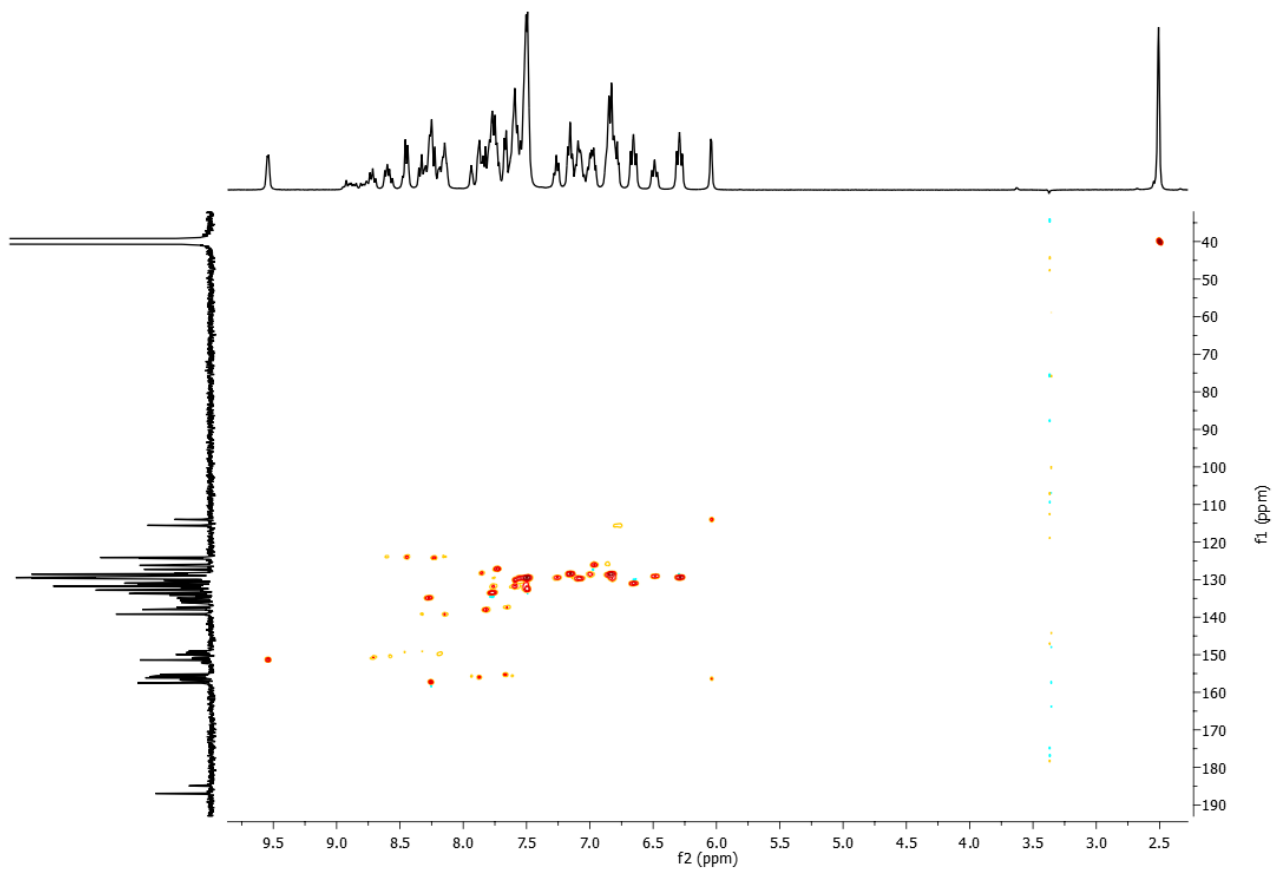


Figure S8. ^1H - ^{13}C HSQC NMR correlation map of complex **2a/2b** in DMSO-d_6 , 298K.

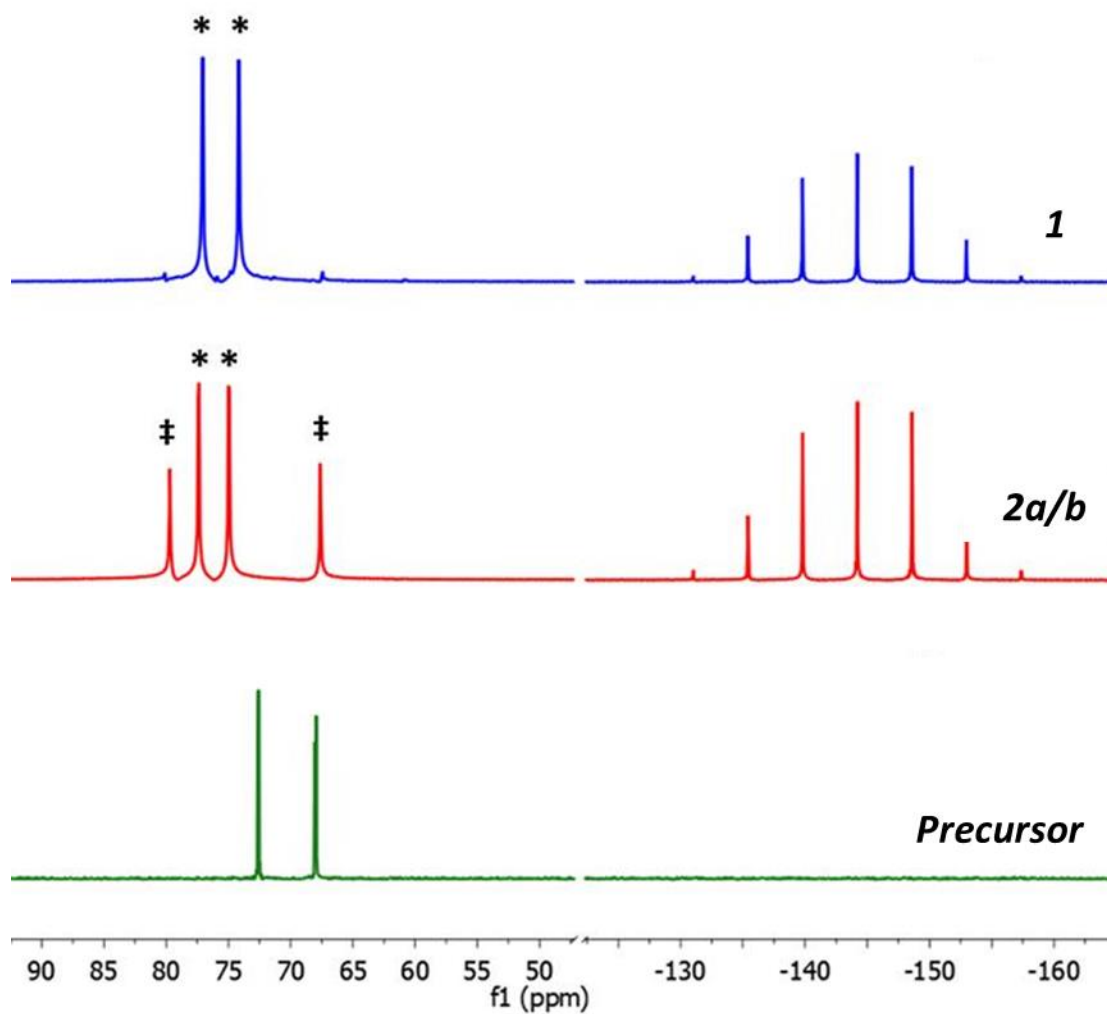


Figure S9. $^{31}\text{P}(^1\text{H})$ NMR spectra of complexes **1**, **2a/2b** and the precursor *cis*-[RuCl₂(bipy)(dppen)] in DCM (in a capillary tube containing D₂O), showing the peak displacement of phosphorus atoms of dppen ligand.

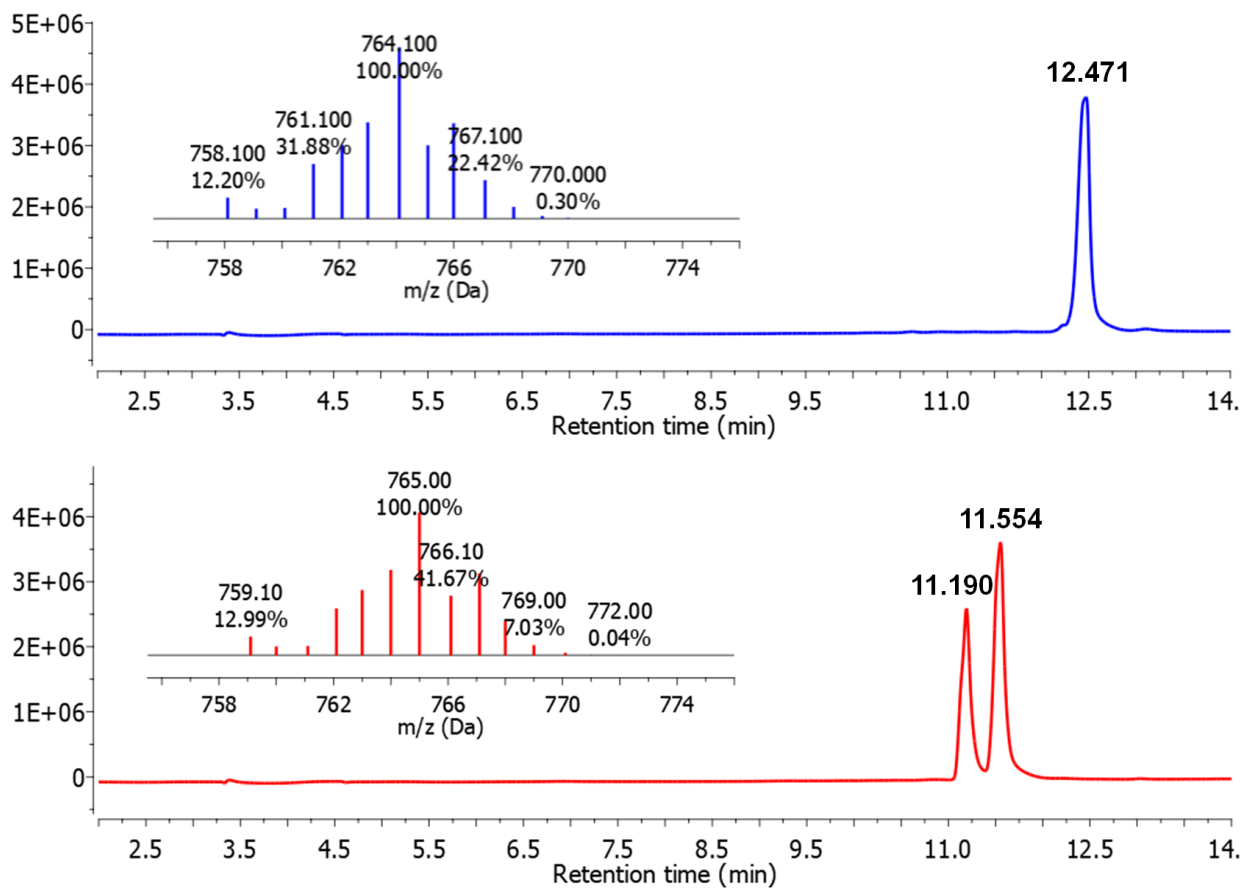


Figure S10. LCMS data: chromatogram and mass spectrum of complexes **1** (top) and **2a/2b** (bottom), in MeOH.

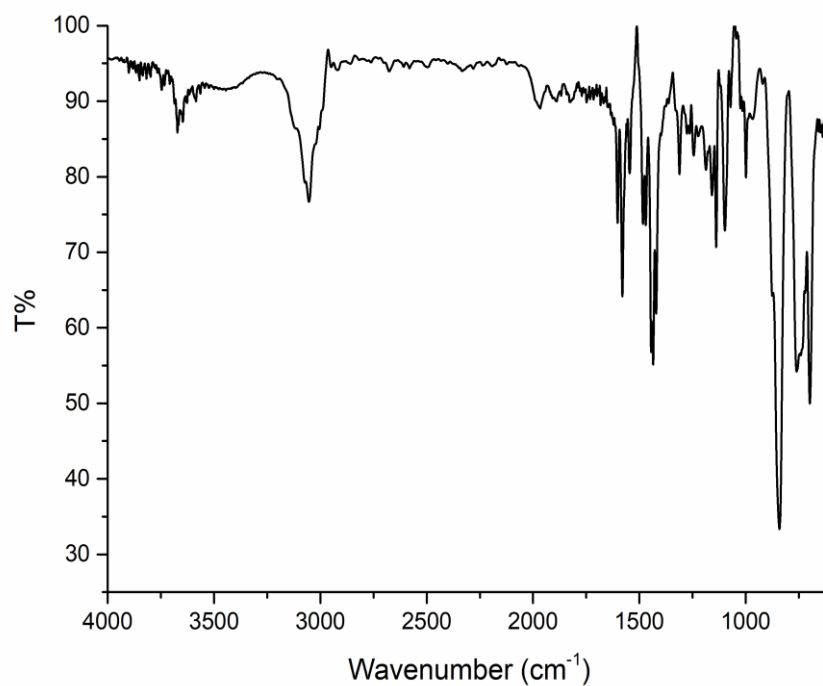


Figure S11. Infrared spectrum (diamond/ZnSe ATR) of complex **1**.

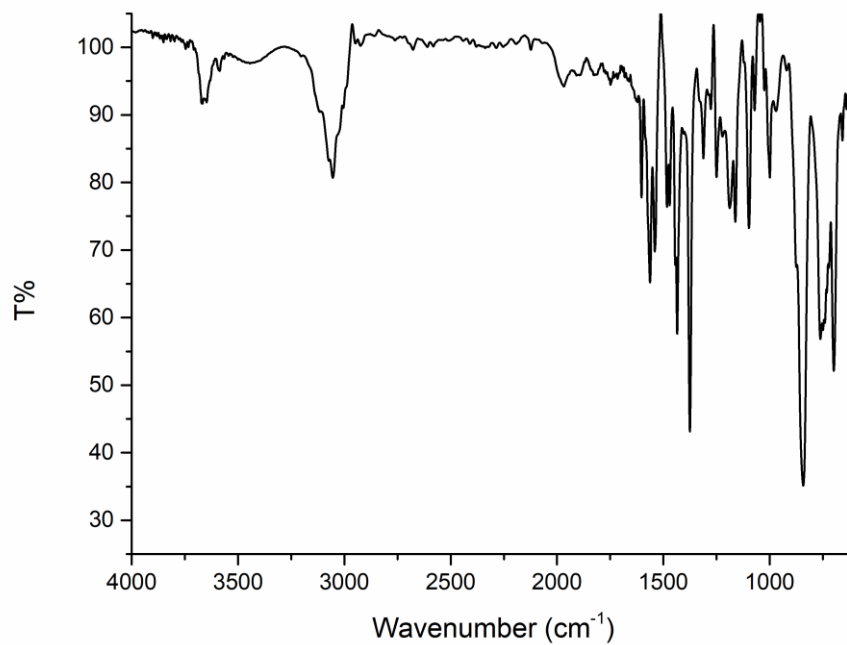


Figure S12. Infrared spectrum (diamond/ZnSe ATR) of complex **2a/2b**.

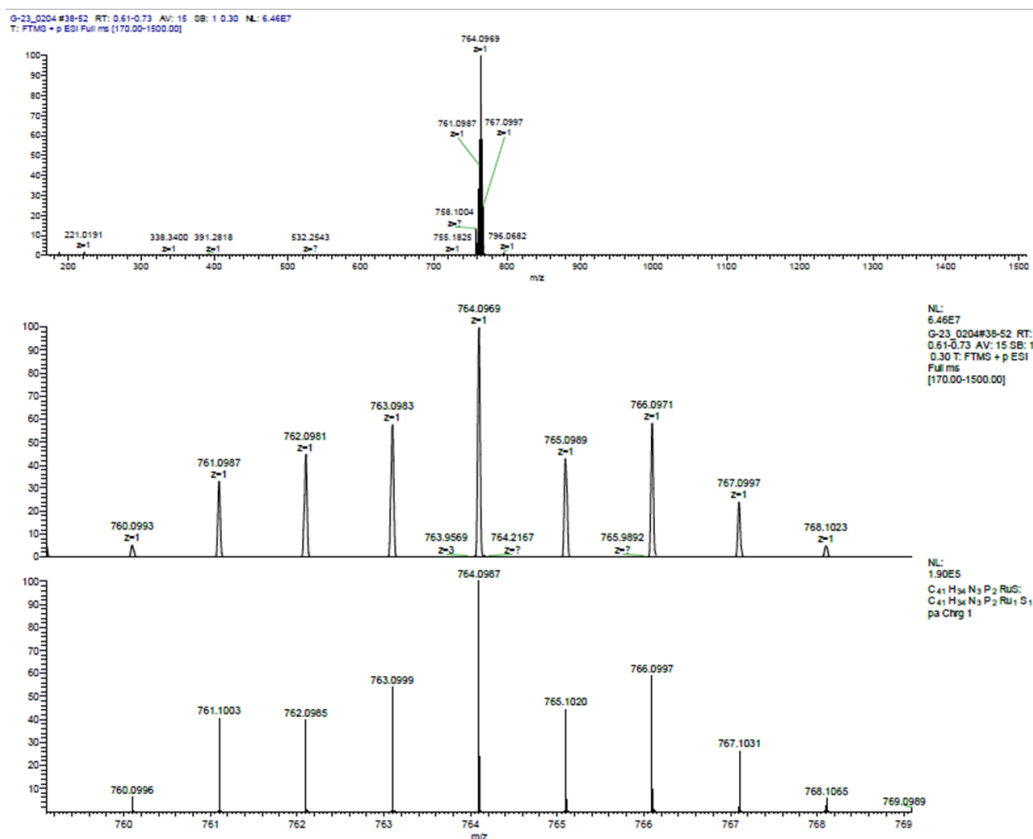


Figure S13. ESI-HRMS data: Full-MS (top) and Experimental/Theoretical isotopic pattern (bottom) MS spectra of complex **1** (positive detection mode in MeOH).

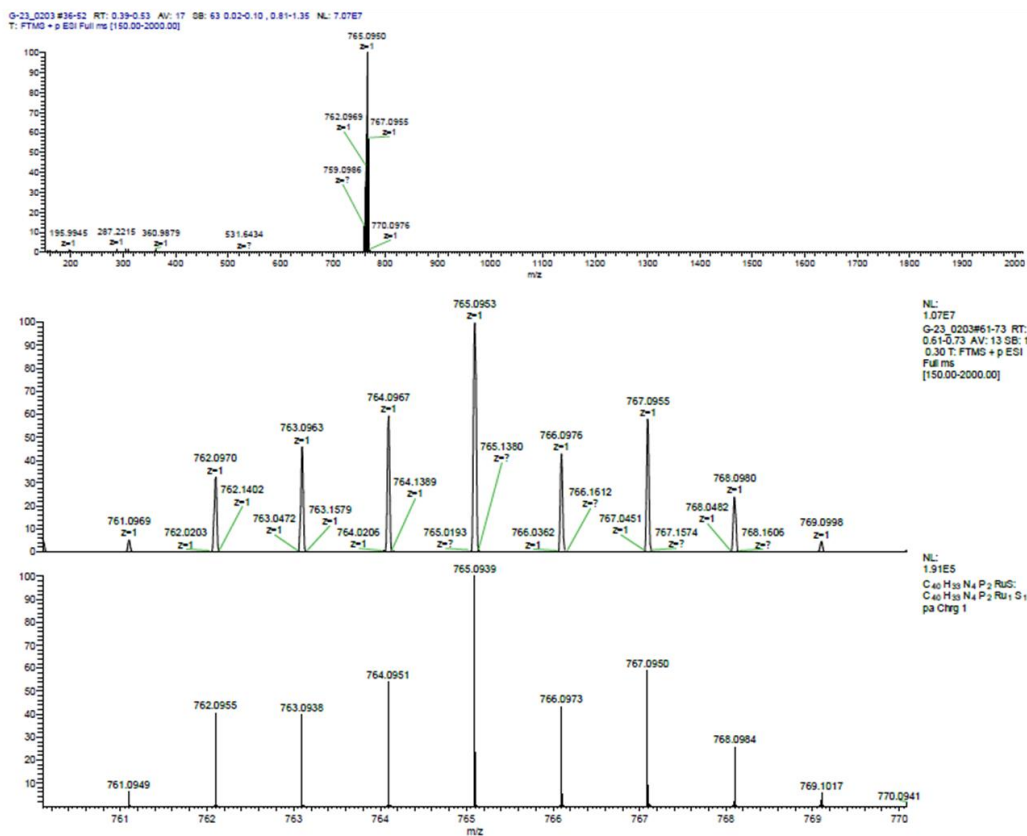


Figure S14. ESI-HRMS data: Full-MS (top) and Experimental/Theoretical isotopic pattern (bottom) MS spectra of complex **2a/2b** (positive detection mode in MeOH).

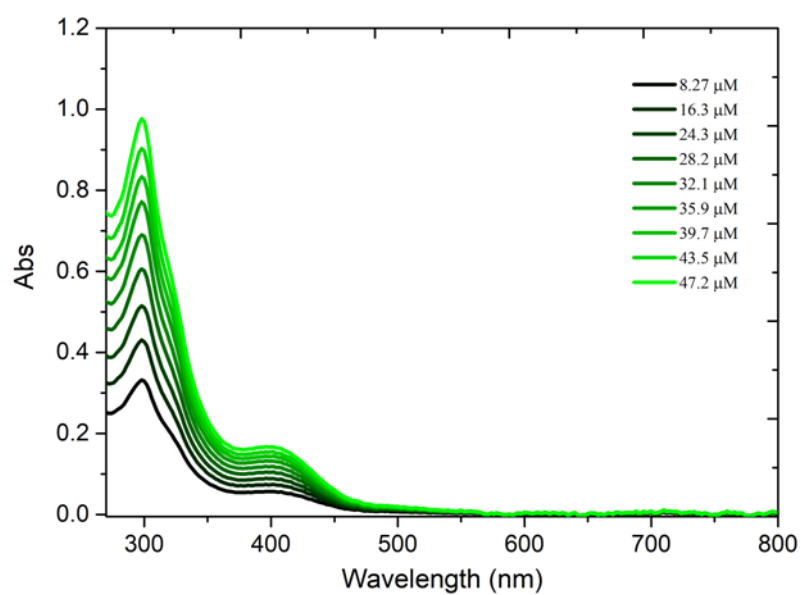
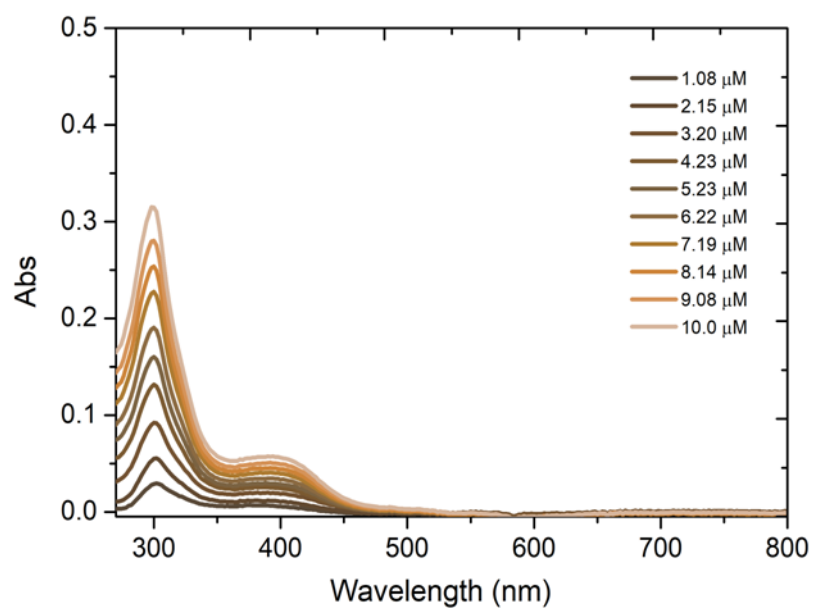


Figure S15. Measured UV-Vis spectra of complex **1** (top) and **2a/2b** (bottom) in DMSO.

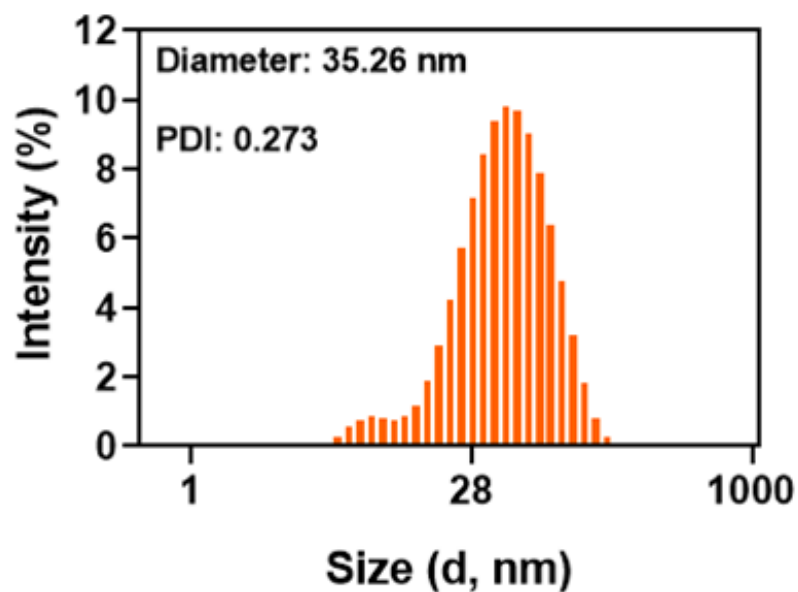


Figure S16. Size distribution by the intensity of complex **2a/2b** (20 μ M) in PBS 10% FBS. Results are presented as mean \pm SD of three independent replicates.

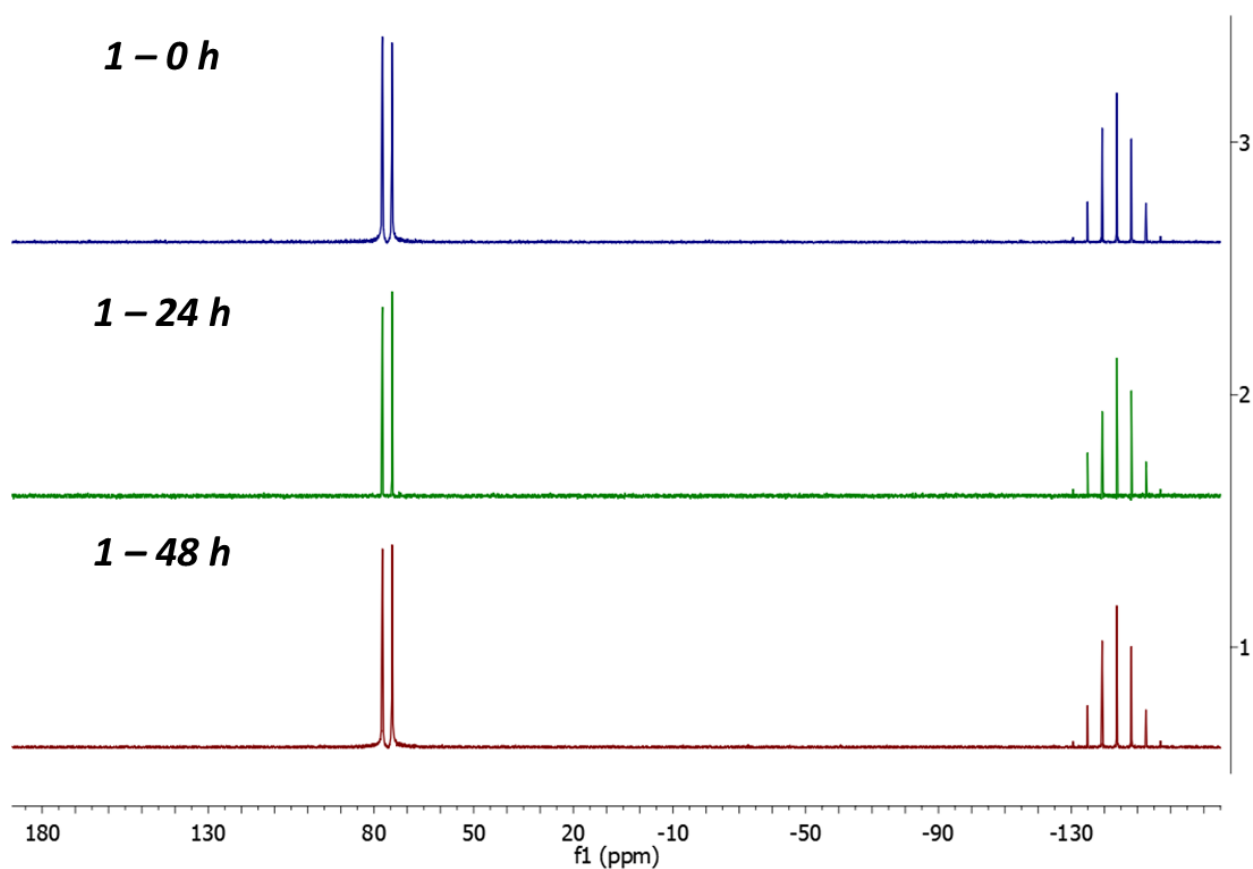


Figure S17. Temporal change of the ^{31}P $\{^1\text{H}\}$ NMR spectra of complex **1** in DMSO/ D_2O during 48 h, at 298 K.

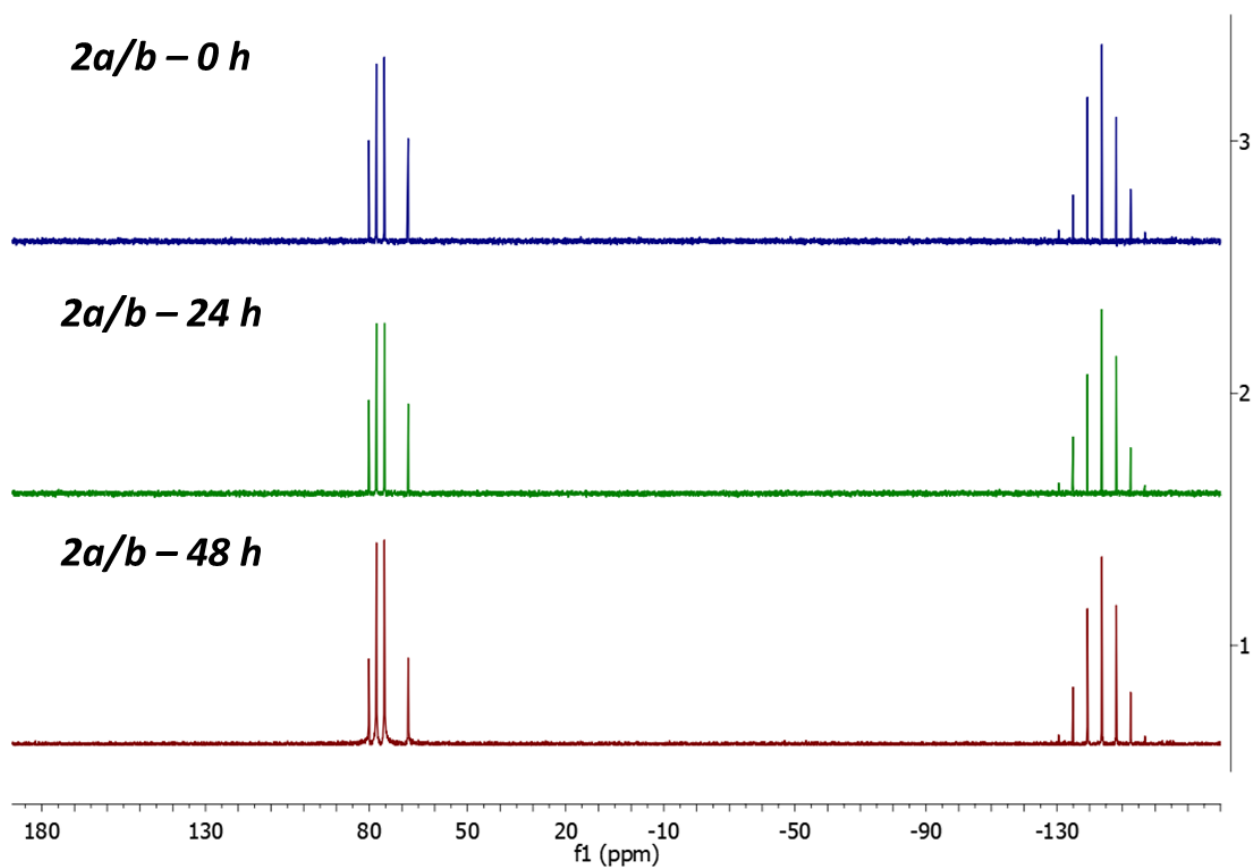


Figure S18. Temporal change of the ^{31}P $\{^1\text{H}\}$ NMR spectra of complex **2a/2b** in DMSO/ D_2O during 48 h, at 298 K.

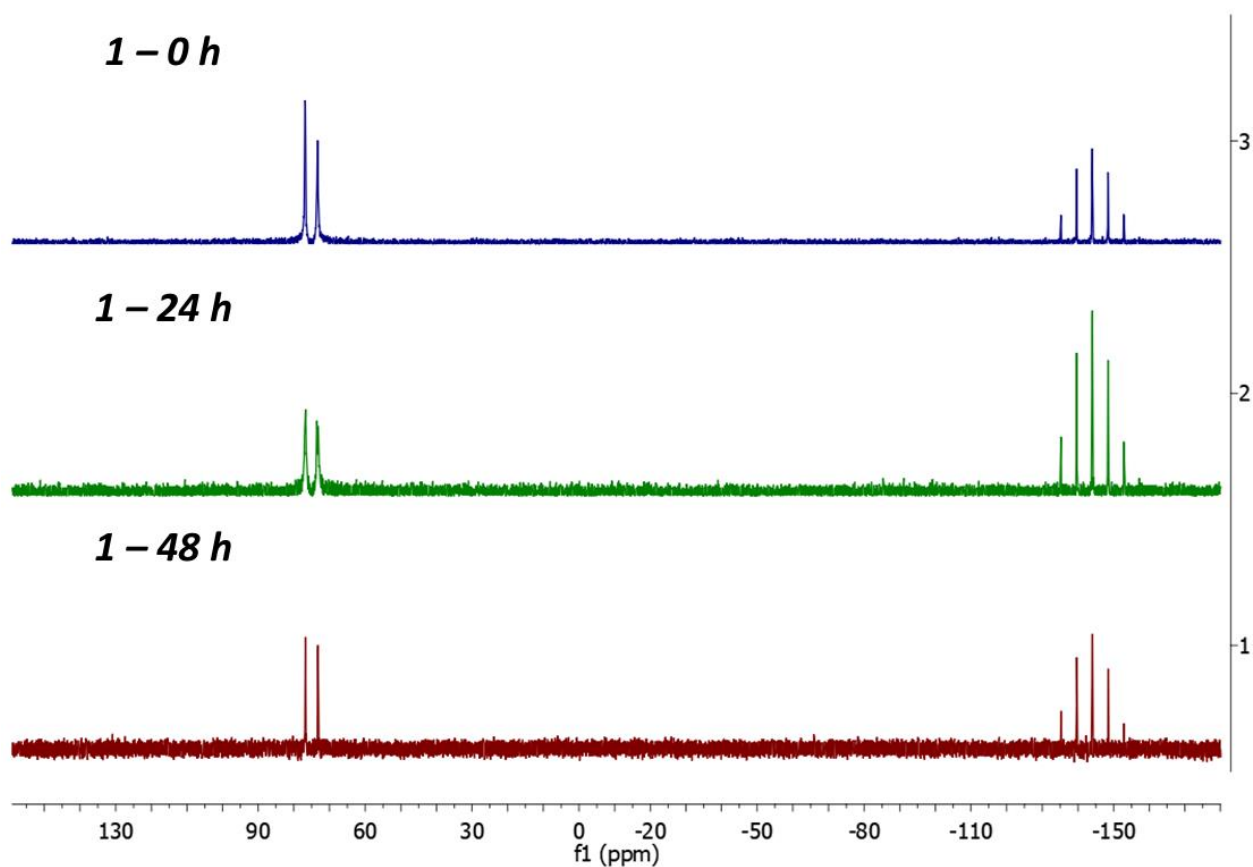


Figure S19. Temporal change of the ^{31}P $\{^1\text{H}\}$ NMR spectra of complex **1** in DMEM (supplemented with 10% fetal bovine serum, 2 mM L-glutamine and 100 U·mL⁻¹ of penicillin-streptomycin mixture) containing 30% DMSO during 48 h, at 298 K.

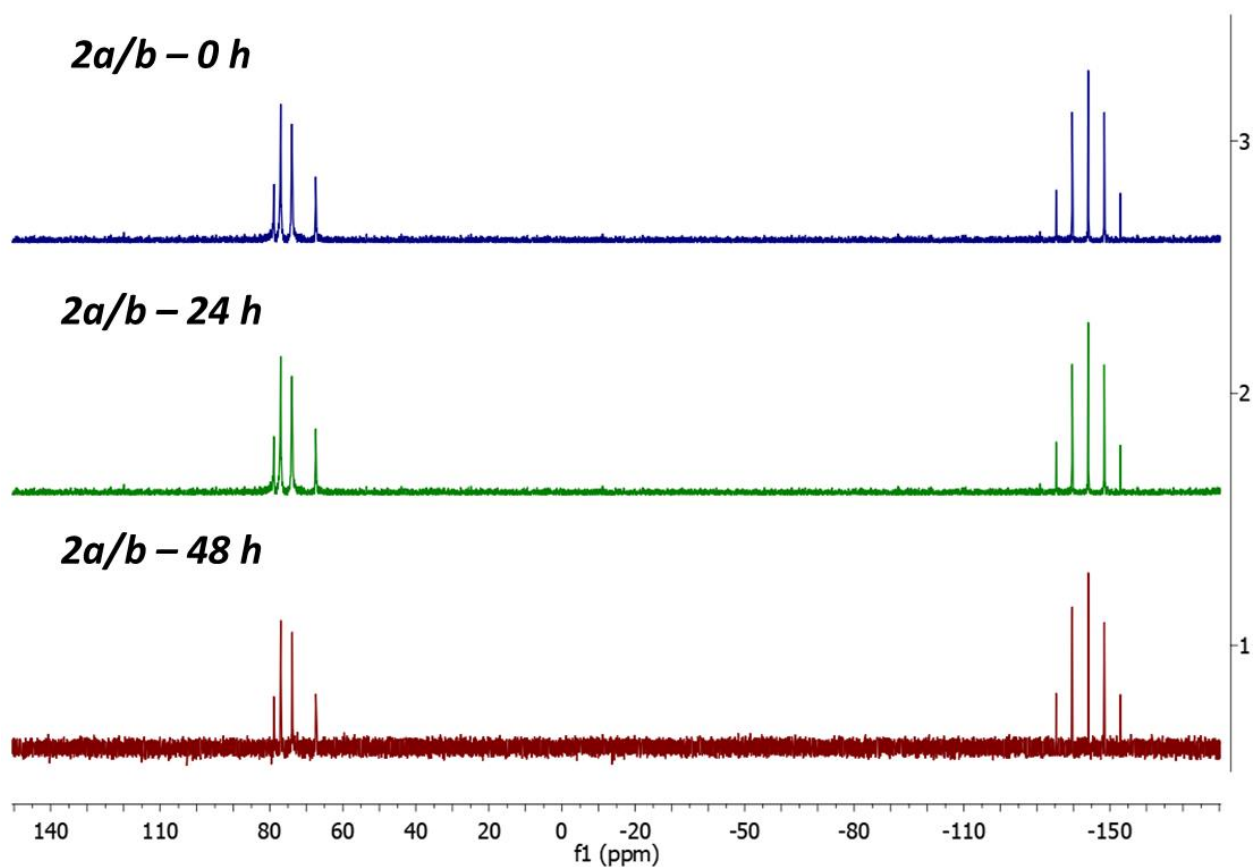


Figure S20. Temporal change of the $^{31}\text{P}\{^1\text{H}\}$ NMR spectra of complex **2a/2b** in DMEM (supplemented with 10% fetal bovine serum, 2 mM L-glutamine and $100\text{ U}\cdot\text{mL}^{-1}$ of penicillin-streptomycin mixture) containing 30% DMSO during 48 h, at 298 K.

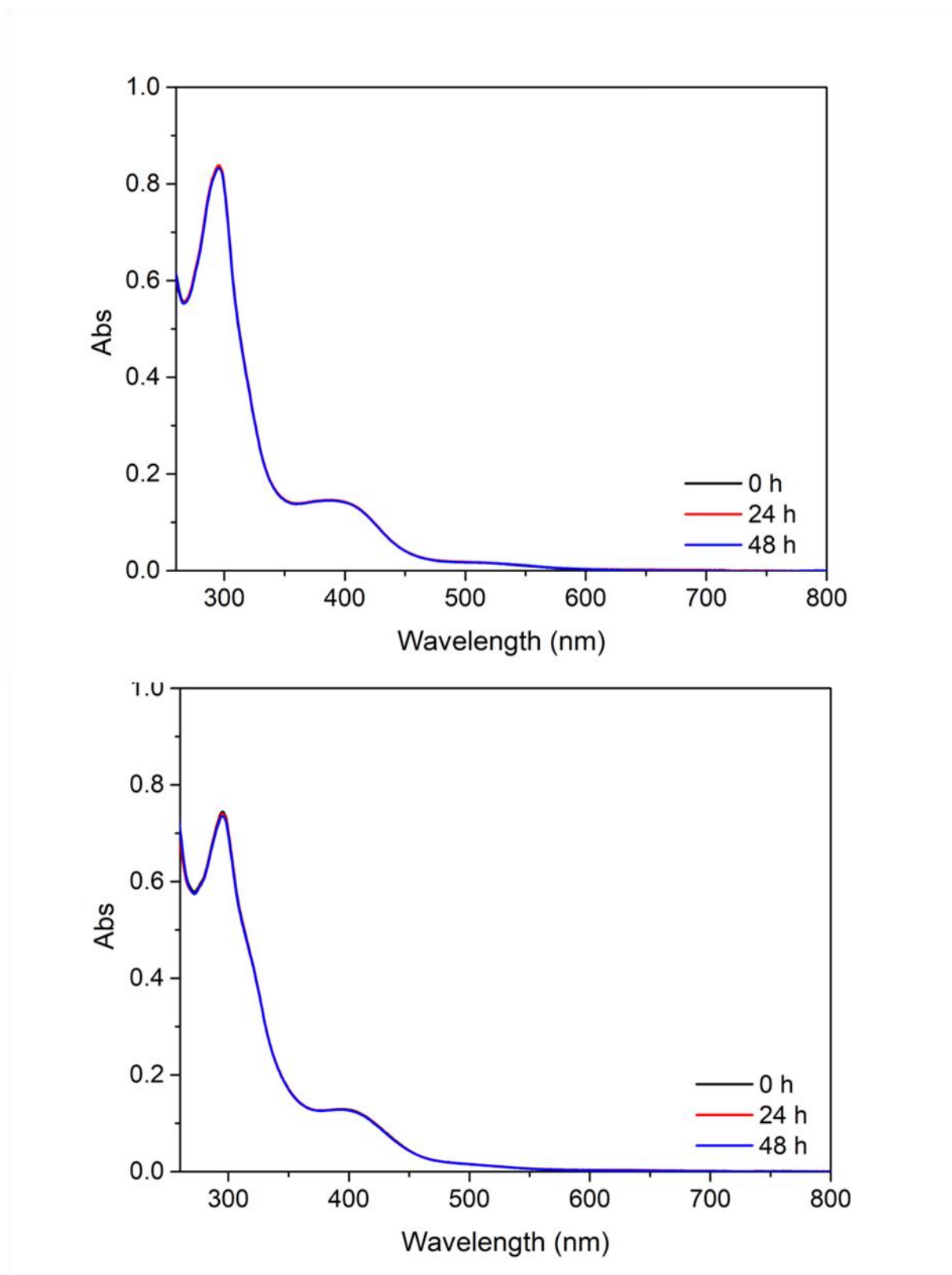


Figure S21. Temporal change of the UV-Vis spectra for 48 h of complexes **1** (top) and **2a/2b** (bottom) in DMSO.

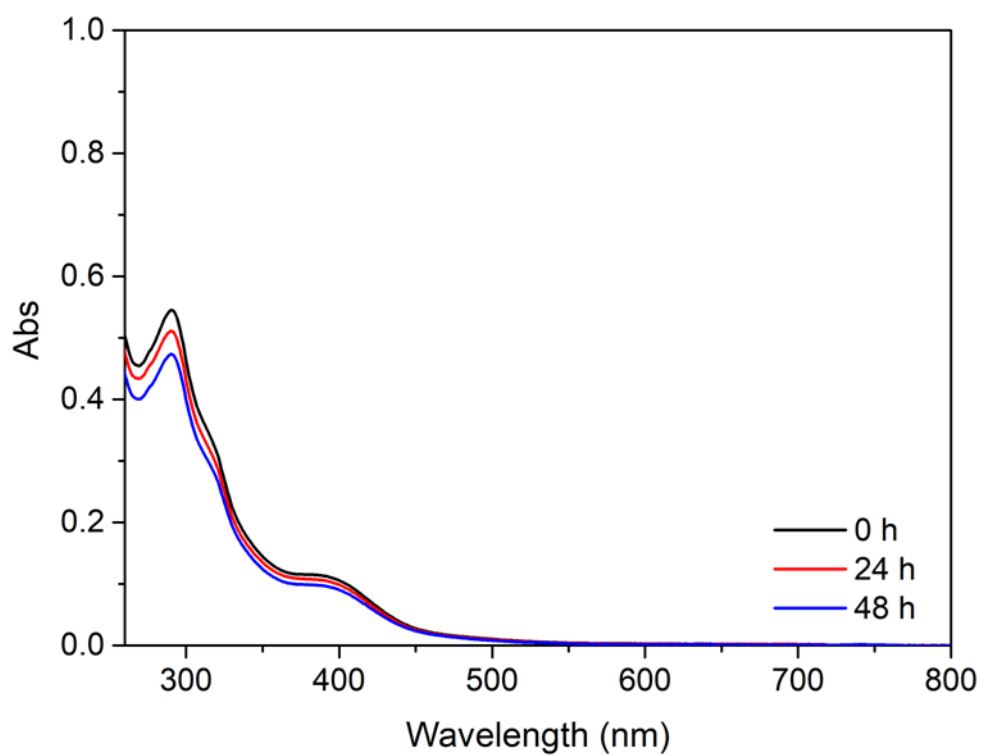
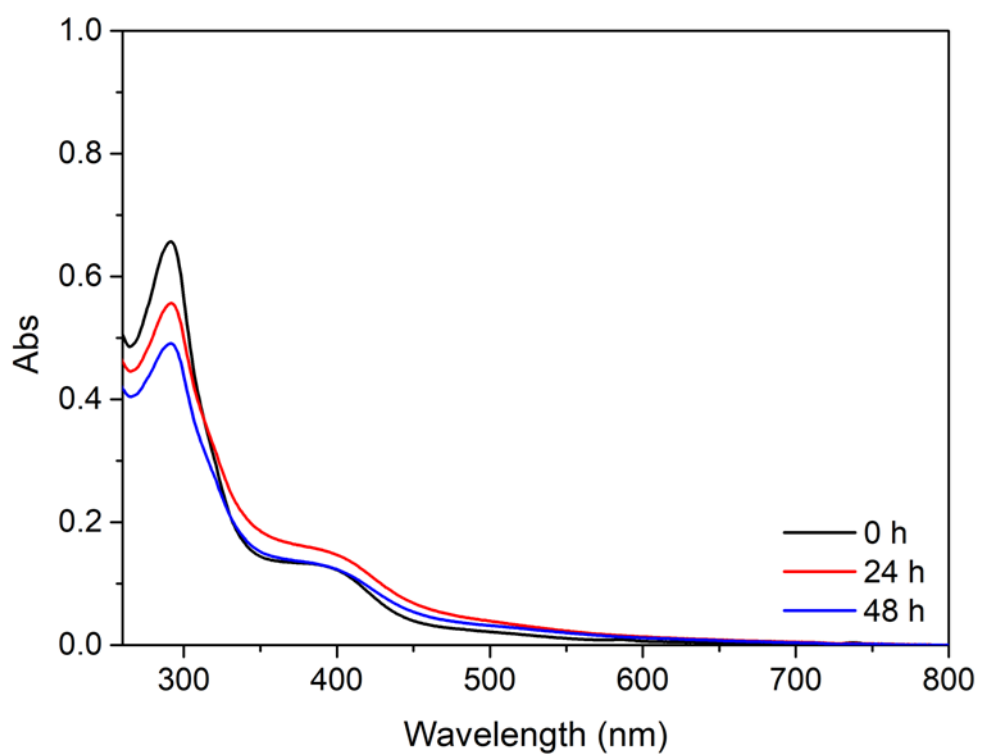


Figure S22. Temporal change of the UV-Vis spectra for 48 h of complexes **1** (top) and **2a/2b** (bottom) in PBS.

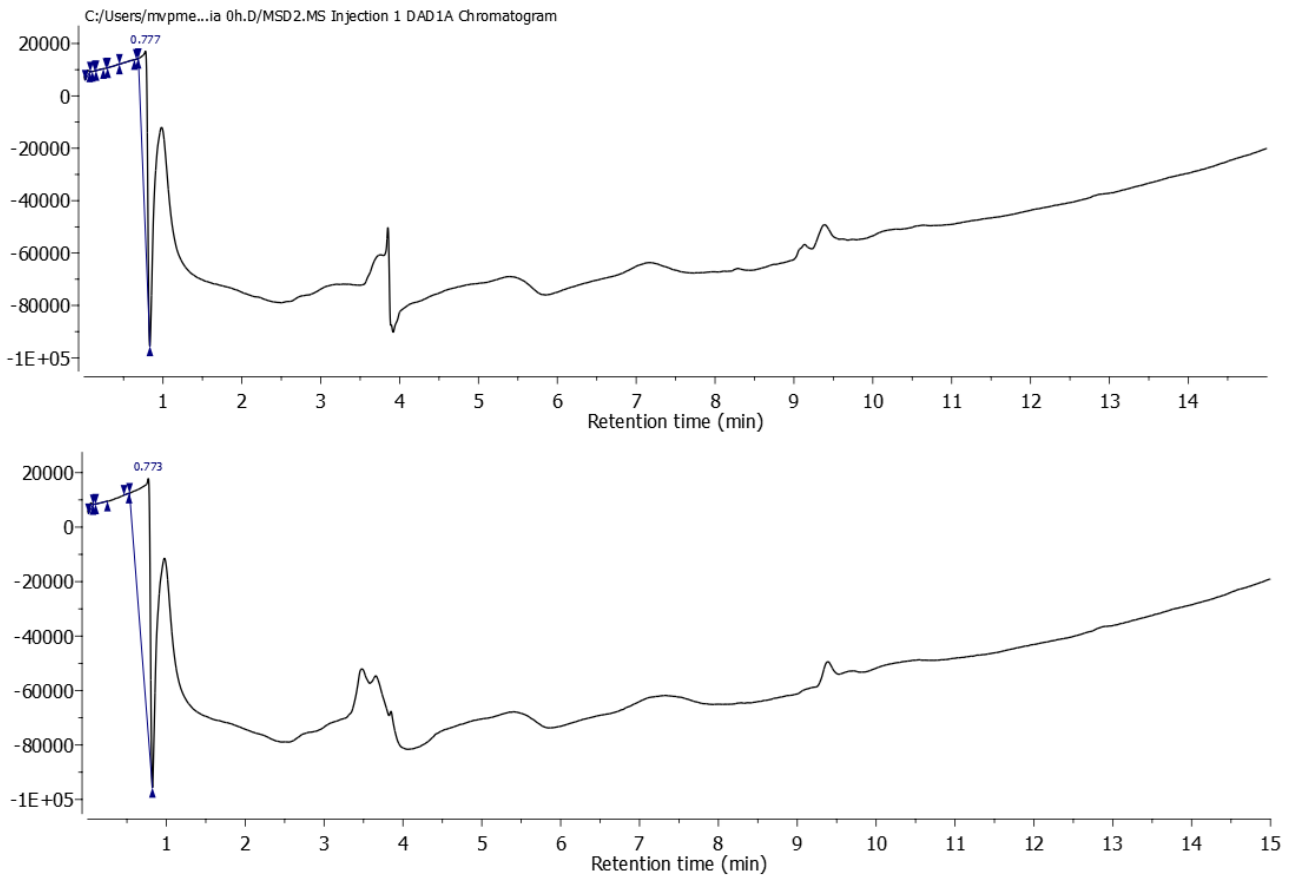


Figure S23. Reversed-phase HPLC traces of cell culture medium/DMSO (DMEM supplemented with 10% fetal bovine serum, 2 mM L-glutamine and 100 U·mL⁻¹ of penicillin-streptomycin mixture) at 250 nm for 0 h and 48 h.

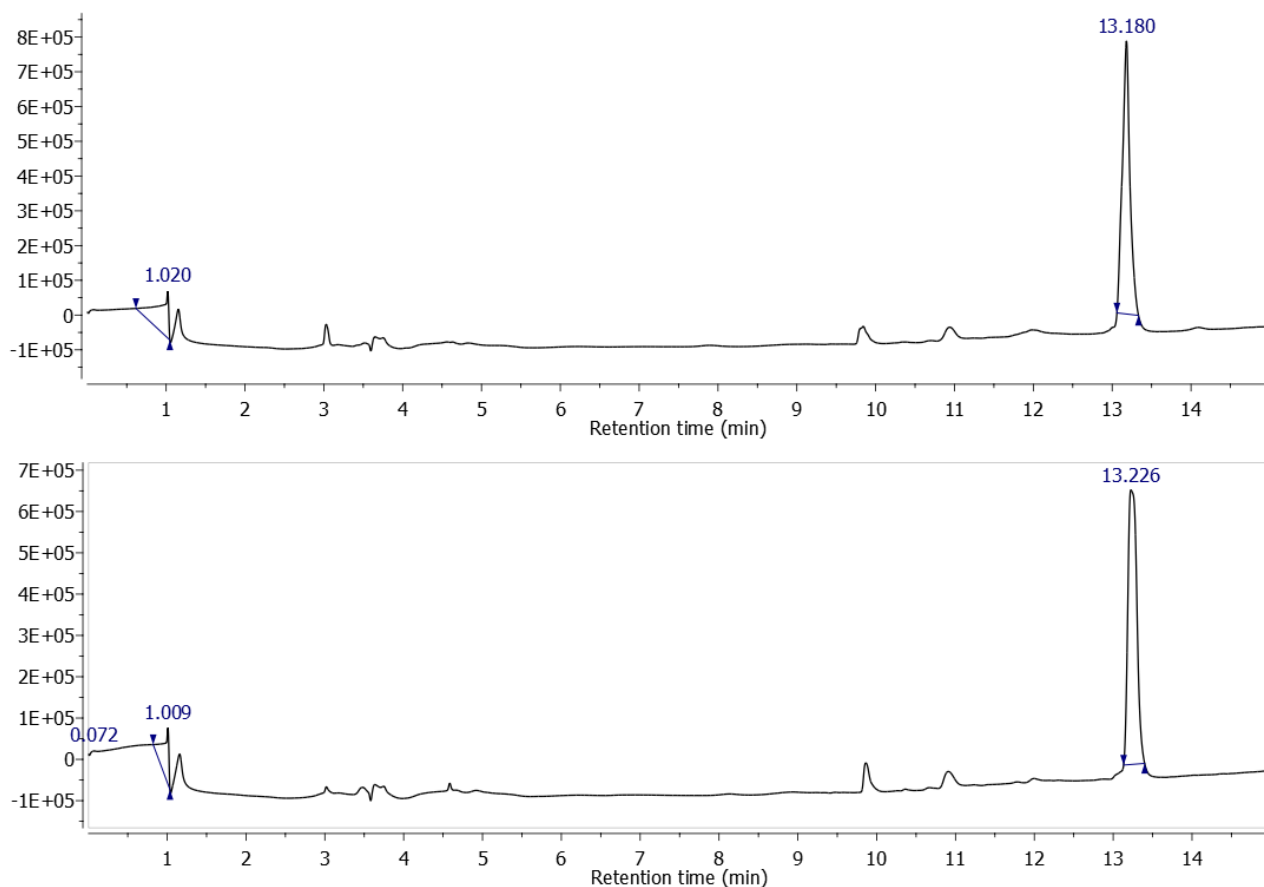


Figure S24. Reversed-phase HPLC traces of complex **1** at 250 nm for 0 h and 48 h in cell culture medium/DMSO (DMEM supplemented with 10% fetal bovine serum, 2 mM L-glutamine and 100 U·mL⁻¹ of penicillin-streptomycin mixture).

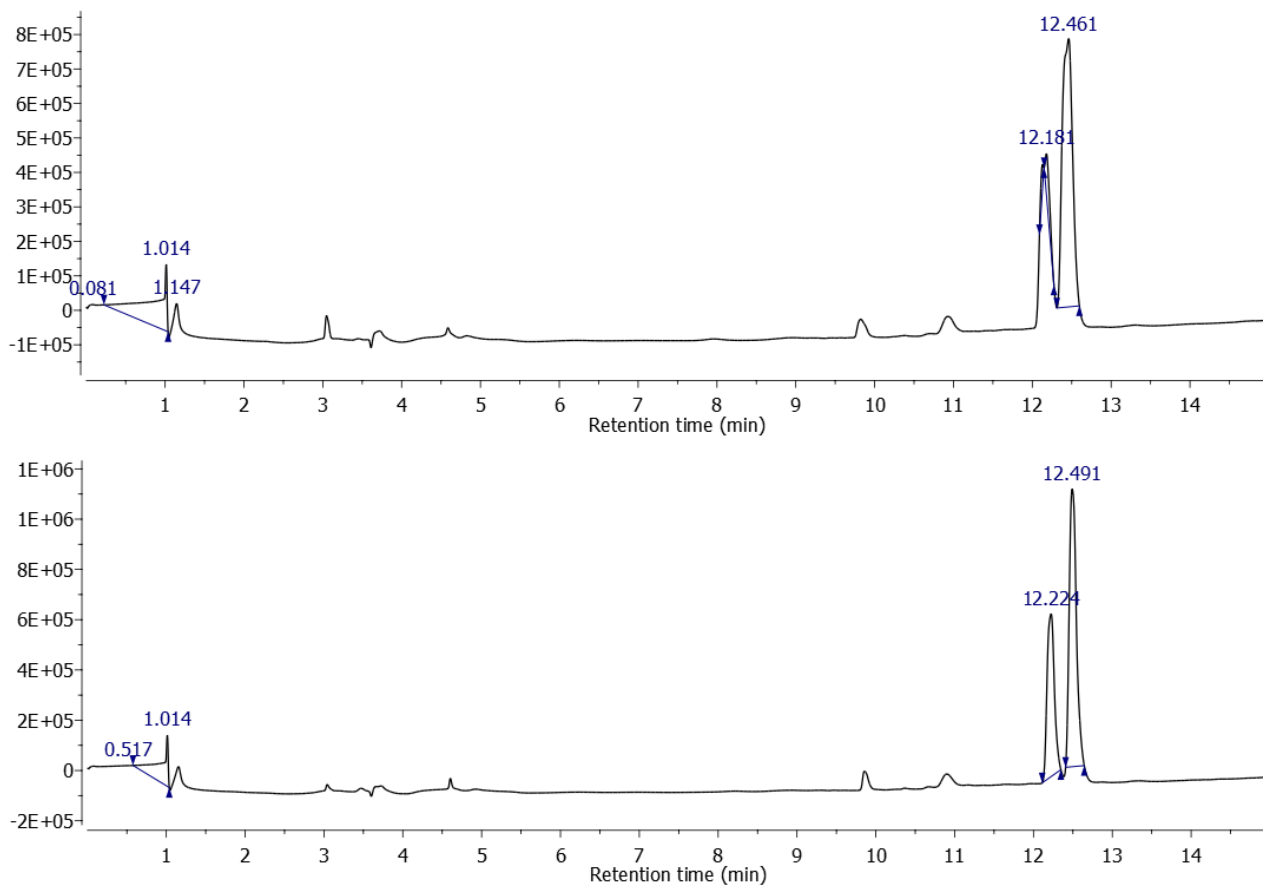


Figure S25. Reversed-phase HPLC traces of complex **2a/2b** at 250 nm for 0 h and 48 h in cell culture medium/DMSO (DMEM supplemented with 10% fetal bovine serum, 2 mM L-glutamine and 100 U·mL⁻¹ of penicillin-streptomycin mixture).

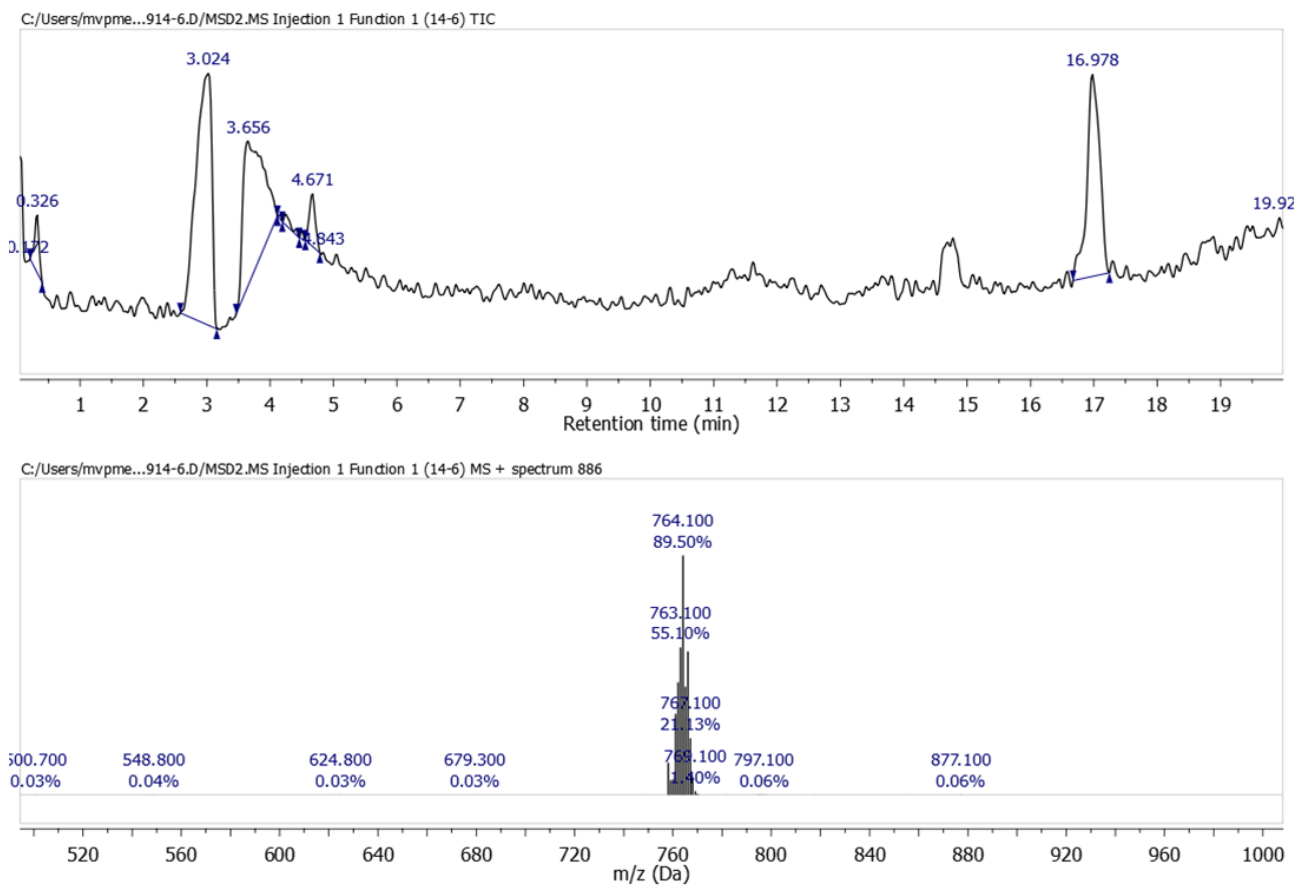


Figure S26. LCMS data: Total ion current (TIC) chromatogram and ESI-MS of complex **1** in PBS/MeOH.

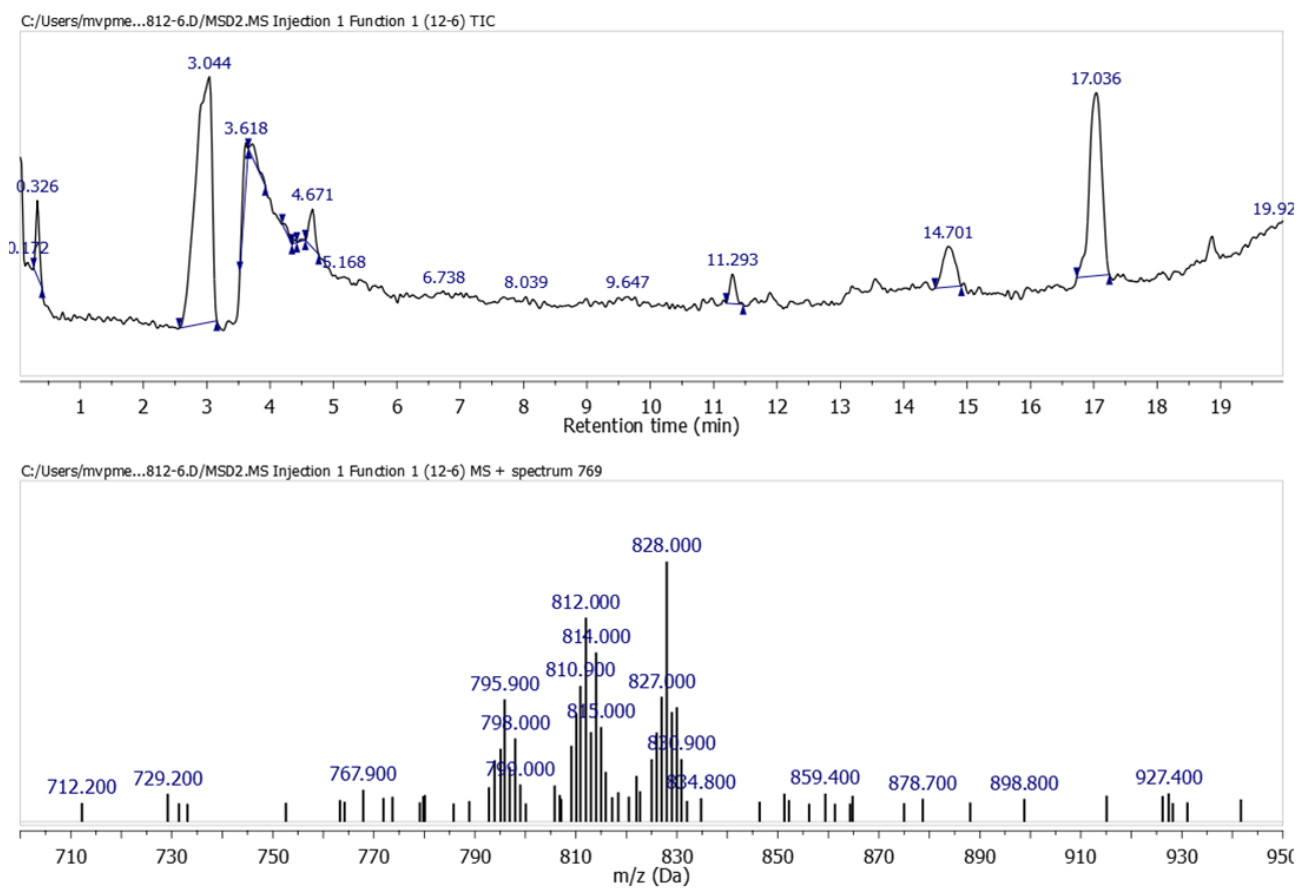


Figure S27. LCMS data: Total ion current (TIC) chromatogram and ESI-MS of complex **1** containing Human Liver Microsomes/NADPH in PBS/MeOH after 6 h incubation.

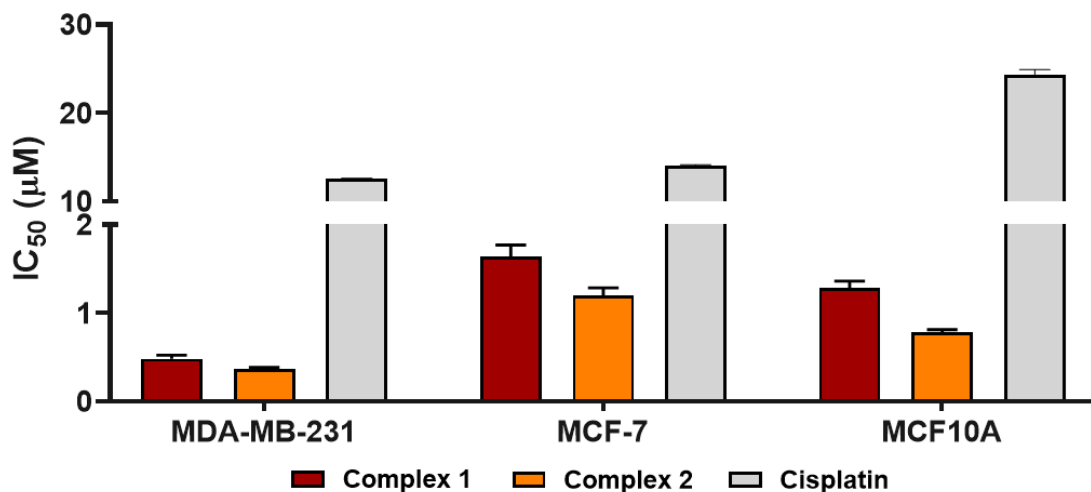


Figure S28. Cytotoxicity (IC_{50} , μM) of complexes **1** and **2a/2b**, and cisplatin against MDA-MB-231 and MCF-7 cancer cells and MCF-10A non-cancerous cells after treatment during 48 h. Data are presented as mean \pm SD of three independent replicates.

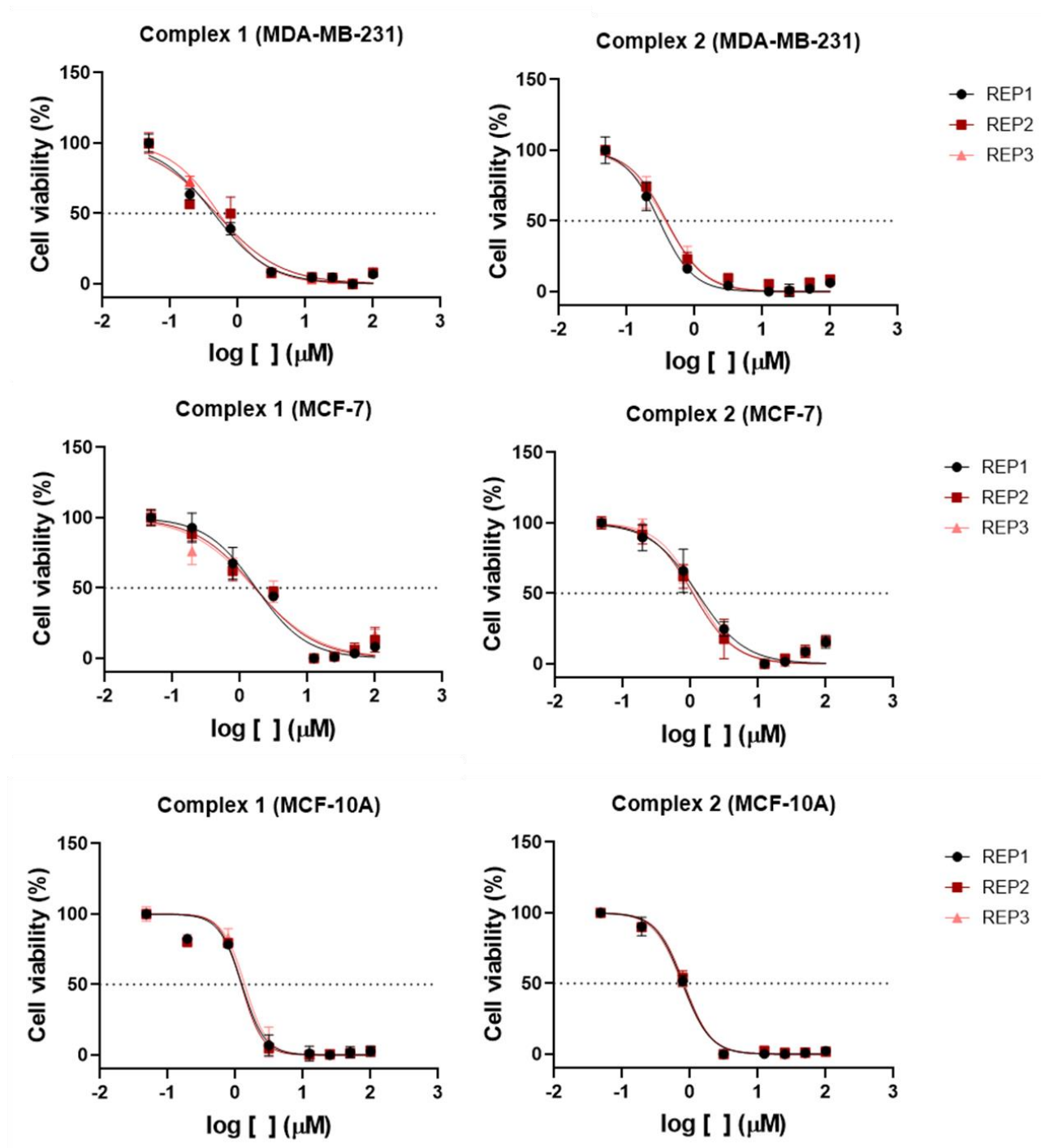


Figure S29. Fluorometric cell viability assay of complexes **1** and **2a/2b** in human breast cancer cells MDA-MB-231 and MCF-7, and non-cancer breast cells MCF-10A after treatment for 48h.

Table S1. The integrated areas of 11.19 and 11.55 min in Figure S10.

Peak #	RetTime [min]	Type	Width [min]	Area [mAU*s]	Height [mAU]	Area %
1	0.041	BB	0.0380	9.12494	3.54743	0.0373
2	0.920	BB	0.2286	1064.44067	55.79627	4.3457
3	1.080	BB	0.2116	635.57629	40.16103	2.5948
4	2.946	BB	0.4987	344.54556	8.14271	1.4066
5	3.381	BB	0.1202	220.91144	26.25071	0.9019
6	4.528	BB	0.3334	267.36765	9.46937	1.0916
7	6.935	BB	0.2512	52.21876	2.45492	0.2132
8	9.325	BB	0.1804	15.04881	1.10810	0.0614
9	10.426	BB	0.1861	17.01336	1.14689	0.0695
10	10.848	BB	0.1486	43.46539	4.00615	0.1775
11	11.192	BB	0.0981	8657.21484	1229.84729	35.3442
12	11.552	BB	0.1186	1.31194e4	1689.88147	53.5616
13	12.210	BB	0.1145	10.13565	1.23838	0.0414
14	13.029	BB	0.1201	37.57490	4.46939	0.1534

Table S2. Crystal data and structure refinement for complex **2b**.

Empirical formula	C ₄₀ H ₃₃ F ₆ N ₄ P ₃ RuS
Formula weight	909.74
Temperature/K	160.0(1)
Crystal system	monoclinic
Space group	P2 ₁ /c
a/Å	8.66950(10)
b/Å	15.33050(10)
c/Å	29.1301(2)
α/°	90
β/°	91.9510(10)
γ/°	90
Volume/Å ³	3869.37(6)
Z	4
ρ _{calc} /g/cm ³	1.562
μ/mm ⁻¹	5.521
F(000)	1840.0
Crystal size/mm ³	0.13 × 0.03 × 0.02
Radiation	Cu Kα (λ = 1.54184)
2θ range for data collection/°	6.072 to 154.732
Index ranges	-10 ≤ h ≤ 10, -19 ≤ k ≤ 14, -36 ≤ l ≤ 28
Reflections collected	46742
Independent reflections	8175 [R _{int} = 0.0281, R _{sigma} = 0.0194]
Data/restraints/parameters	8175/0/496
Goodness-of-fit on F ²	1.057
Final R indexes [I ≥ 2σ (I)]	R ₁ = 0.0236, wR ₂ = 0.0614
Final R indexes [all data]	R ₁ = 0.0252, wR ₂ = 0.0622
Largest diff. peak/hole / e Å ⁻³	0.45/-0.56

Table S3. Bond Lengths for complex **2b**.

Atom	Atom	Length/Å	Atom	Atom	Length/Å
C1	C2	1.385(3)	C24	C25	1.377(3)
C1	N1	1.337(2)	C25	C26	1.383(3)
C2	C3	1.379(4)	C27	C28	1.322(2)
C3	N2	1.338(3)	C27	P1	1.8132(17)
C4	N1	1.364(2)	C28	P2	1.8142(17)
C4	N2	1.332(2)	C29	C30	1.395(2)
C4	S1	1.7296(19)	C29	C34	1.385(3)
C5	C6	1.382(2)	C29	P2	1.8306(16)
C5	N3	1.347(2)	C30	C31	1.395(3)
C6	C7	1.375(3)	C31	C32	1.372(3)
C7	C8	1.381(3)	C32	C33	1.385(3)
C8	C9	1.390(2)	C33	C34	1.394(3)
C9	C10	1.472(2)	C35	C36	1.388(3)
C9	N3	1.352(2)	C35	C40	1.387(3)
C10	C11	1.391(2)	C35	P2	1.8317(18)
C10	N4	1.365(2)	C36	C37	1.388(3)
C11	C12	1.382(3)	C37	C38	1.376(3)
C12	C13	1.379(3)	C38	C39	1.384(4)
C13	C14	1.383(3)	C39	C40	1.387(3)
C14	N4	1.347(2)	N1	Ru1	2.0817(14)
C15	C16	1.397(2)	N3	Ru1	2.1219(13)
C15	C20	1.393(3)	N4	Ru1	2.0898(13)
C15	P1	1.8246(17)	P1	Ru1	2.2736(4)
C16	C17	1.389(3)	P2	Ru1	2.2813(4)
C17	C18	1.375(3)	Ru1	S1	2.4602(4)
C18	C19	1.376(3)	F1	P3	1.5951(14)
C19	C20	1.390(3)	F2	P3	1.6061(16)

Atom	Atom	Length/Å	Atom	Atom	Length/Å
C21	C22	1.395(2)	F3	P3	1.6095(15)
C21	C26	1.396(2)	F4	P3	1.5843(16)
C21	P1	1.8273(18)	F5	P3	1.5997(13)
C22	C23	1.384(3)	F6	P3	1.5917(16)
C23	C24	1.385(3)			

Table S4. Bond Angles for complex **2b**.

Atom	Atom	Atom	Angle/°	Atom	Atom	Atom	Angle/°
N1	C1	C2	120.5(2)	C1	N1	C4	117.98(16)
C3	C2	C1	117.0(2)	C1	N1	Ru1	139.26(14)
N2	C3	C2	124.07(19)	C4	N1	Ru1	102.45(11)
N1	C4	S1	110.34(12)	C4	N2	C3	115.30(19)
N2	C4	N1	125.09(17)	C5	N3	C9	118.47(14)
N2	C4	S1	124.56(15)	C5	N3	Ru1	126.10(12)
N3	C5	C6	122.92(17)	C9	N3	Ru1	115.42(10)
C7	C6	C5	118.31(17)	C10	N4	Ru1	115.56(10)
C6	C7	C8	119.79(17)	C14	N4	C10	117.41(14)
C7	C8	C9	119.18(17)	C14	N4	Ru1	127.01(11)
C8	C9	C10	123.50(16)	C15	P1	C21	105.46(8)
N3	C9	C8	121.31(15)	C15	P1	Ru1	118.28(6)
N3	C9	C10	115.17(14)	C21	P1	Ru1	117.69(6)
C11	C10	C9	122.25(15)	C27	P1	C15	103.12(8)
N4	C10	C9	115.98(14)	C27	P1	C21	100.77(8)
N4	C10	C11	121.71(15)	C27	P1	Ru1	109.20(6)
C12	C11	C10	119.66(17)	C28	P2	C29	103.60(8)
C13	C12	C11	118.86(17)	C28	P2	C35	102.24(8)
C12	C13	C14	118.99(16)	C28	P2	Ru1	109.14(5)

Atom Atom Atom Angle/°				Atom Atom Atom Angle/°			
N4	C14	C13	123.29(16)	C29	P2	C35	101.72(8)
C16	C15	P1	119.44(14)	C29	P2	Ru1	122.90(6)
C20	C15	C16	118.87(16)	C35	P2	Ru1	114.87(5)
C20	C15	P1	121.43(13)	N1	Ru1	N3	90.78(5)
C17	C16	C15	120.43(18)	N1	Ru1	N4	163.18(5)
C18	C17	C16	119.90(19)	N1	Ru1	P1	103.36(4)
C17	C18	C19	120.45(19)	N1	Ru1	P2	90.09(4)
C18	C19	C20	120.2(2)	N1	Ru1	S1	67.66(4)
C19	C20	C15	120.14(18)	N3	Ru1	P1	95.20(4)
C22	C21	C26	118.51(17)	N3	Ru1	P2	178.83(4)
C22	C21	P1	119.45(13)	N3	Ru1	S1	88.17(4)
C26	C21	P1	121.94(14)	N4	Ru1	N3	77.80(5)
C23	C22	C21	120.58(17)	N4	Ru1	P1	90.09(4)
C22	C23	C24	120.19(19)	N4	Ru1	P2	101.52(4)
C25	C24	C23	119.77(19)	N4	Ru1	S1	99.30(4)
C24	C25	C26	120.42(18)	P1	Ru1	P2	83.836(14)
C25	C26	C21	120.54(18)	P1	Ru1	S1	170.509(15)
C28	C27	P1	118.57(13)	P2	Ru1	S1	92.882(14)
C27	C28	P2	118.07(13)	C4	S1	Ru1	78.99(6)
C30	C29	P2	121.51(14)	F1	P3	F2	89.67(9)
C34	C29	C30	119.03(16)	F1	P3	F3	178.68(10)
C34	C29	P2	119.43(13)	F1	P3	F5	89.90(7)
C31	C30	C29	120.20(18)	F2	P3	F3	89.01(9)
C32	C31	C30	120.05(18)	F4	P3	F1	91.08(9)
C31	C32	C33	120.48(18)	F4	P3	F2	178.74(10)
C32	C33	C34	119.6(2)	F4	P3	F3	90.24(9)
C29	C34	C33	120.64(18)	F4	P3	F5	90.11(8)
C36	C35	P2	120.26(14)	F4	P3	F6	90.40(10)

Atom Atom Atom Angle/°				Atom Atom Atom Angle/°			
C40	C35	C36	119.22(18)	F5	P3	F2	88.88(8)
C40	C35	P2	120.24(14)	F5	P3	F3	90.09(8)
C35	C36	C37	120.34(19)	F6	P3	F1	89.85(9)
C38	C37	C36	120.1(2)	F6	P3	F2	90.61(10)
C37	C38	C39	120.1(2)	F6	P3	F3	90.16(9)
C38	C39	C40	119.9(2)	F6	P3	F5	179.43(9)
C35	C40	C39	120.3(2)				

Table S5. Areas of complex **1** at 16.98 and 17.00 min in Figure 5 (a and c).

Time	Area	Height	Width
16.98	279.54761	35.66253	0.1175
17.00	242.34882	29.76770	0.1170